

Supplementary Information

Interfacial Electronic Tuning of Pt-Co₃O₄ Enables Highly Efficient Electrocatalytic Hydrogenation of Phenol

FenHong Zhao,^a Yue Wang,^a Long Chen,^a MengYv Guo,^a Xuejun Liu^{*,a,b,c,d} Fengshan Zhang,^{*,b,c,d}
and Lixue Zhang,^a

^a College of Chemistry and Chemical Engineering, Qingdao University, Qingdao, 266071, China

^b Shandong Key Laboratory of Biobased Material and Green Pulp Papermaking, Dongying 257335,
China

^c Shandong Huatai Paper Co., Ltd. Dongying 257335, China

^d Shandong Yellow Triangle Biotechnology Industry Research Institute Co., Ltd., Dongying
257000, China

Corresponding author: htjszx@163.com; xjliu@qdu.edu.cn

1. Experimental Section

1.1. Materials

phenol (C_6H_5OH , GC, $\geq 99.5\%$), Cobalt nitrate, hexahydrate ($Co(NO_3)_2 \cdot 6H_2O$, AR, 99%), Dichloromethane (CH_2Cl_2 , GC, $\geq 99.8\%$), and sodium sulfate anhydrous (Na_2SO_4 , GC, $\geq 99.0\%$) were purchased from Shanghai Aladdin Biochemical Technology Co., Ltd. Cyclohexanol ($C_6H_{12}O$, GC, 98.5%) was purchased from Shanghai Macklin Biochemical Co., Ltd. Chloroplatinic acid hexahydrate ($H_2PtCl_6 \cdot 6H_2O$, AR, $> 37\%$), sulphuric acid (H_2SO_4 , AR, 98%), nitric acid (HNO_3 , AR), hydrogen peroxide (H_2O_2 , $\geq 30\%$), and ethanol (C_2H_5OH , AR, $\geq 99.7\%$) were bought from Sinopharm Chemical Reagent Co., Ltd. Cyclohexanone ($C_6H_{10}O$, GC, $\geq 99.5\%$) was purchased from Sigma-Aldrich Chemical Reagent Co., Ltd. Carbon cloth (CC, HCP 330N) was purchased from Suzhou Sinero Technology Co., Ltd. Nafion solution (5%) was purchased from Dupont Corporation. Proton exchange membrane (Nafion N117) was purchased from Wuhan Gaoss Union Technology Co., Ltd. All the reagents were used as received without further purification. Deionized water (resistivity $> 18.2 M\Omega$) was used to prepare the aqueous solution.)

2. Catalyst synthesis

Pre-treatment of carbon cloth (CC)

Typically, the carbon cloth (CC) was placed in a reactor containing 30 mL HNO_3 and heated in an oven at $120\text{ }^\circ\text{C}$ for 2 h. After cooling to room temperature, the treated CC was ultrasonically cleaned in anhydrous ethanol and deionized water for several times, respectively, and dried at $60\text{ }^\circ\text{C}$.

The synthesis of Co_3O_4/CC

Firstly, the $Co(OH)_2$ nanosheet arrays grown on CC were prepared by electrochemical deposition. Specially, the CC ($1.5\text{ cm} \times 2.5\text{ cm}$), a platinum plate and a saturated calomel electrode (SCE) were used as a substrate, counter electrode and reference electrode, respectively. The 25 mM $Co(NO_3)_2$ solution was put in a beaker, and the CC was placed on an electrode clamp and immersed in the solution, keeping that the immersed area of CC in solution is $1.5\text{ cm} \times 2.5\text{ cm}$. The blue $Co(OH)_2$ was obtained after working at -1 V vs. SCE for 240 s, and then it was placed in a tubular furnace to obtain Co_3O_4 via

controlling the calcination temperature. After the as-prepared $\text{Co}(\text{OH})_2$ was calcined at $400\text{ }^\circ\text{C}$ for 2 h with a heating rate of $2\text{ }^\circ\text{C min}^{-1}$ in air, the Co_3O_4 could be obtained.

The synthesis of Pt- $\text{Co}_3\text{O}_4/\text{CC}$

Pt was deposited onto $\text{Co}_3\text{O}_4/\text{CC}$ via electrodeposition, which was carried out in a three-electrode electrochemical cell. A platinum sheet and an Ag/AgCl electrode (saturated with KCl) were used as the counter electrode and reference electrode, respectively. The substrate was subjected to 10 cycles of cyclic voltammetry (CV) deposition at a scan rate of $0.1\text{ V}\cdot\text{s}^{-1}$ within a potential range of -0.5 to 1.7 V. The electrolyte was prepared using an aqueous solution containing 0.5 M Na_2SO_4 and 10 mM H_2PtCl_6 . After electrodeposition, the working electrode was rinsed with distilled water and dried at room temperature under atmospheric pressure. For comparison, the controlled samples were obtained following the similar process except the change of CV deposition cycles.

3. Electrochemical Measurements

The electrochemical measurements were carried out with Bio-Logic VSP-300 workstation at room temperature. The HER and phenol ECH measurements were conducted in an H-cell reactor with two compartments separated by a Nafion 117 proton exchange membrane. The cathode chamber was filled with 23 mL aqueous solution containing 0.1 M H_2SO_4 and 10 mM phenol, while the anode chamber was filled with 23 mL 0.1 M H_2SO_4 aqueous solution. Argon (Ar) gas was continuously purged into the electrolyte before 20 min the tests. The standard three-electrode setup with the as-synthesized catalysts as the working electrode ($1.5\text{ cm}\times 2.5\text{ cm}$), a graphite rod as the counter electrode, and a Hg/Hg₂SO₄ (sat. K₂SO₄) as the reference electrode was employed. Linear sweep voltammetry (LSV) was collected with a 5 mV s^{-1} sweep rate in 0.1 M H_2SO_4 solution with and without 10 mM phenol. All the potentials in this study were converted to RHE reference scale using the following equation:

$$E_{RHE} = E_{\text{Hg}/\text{Hg}_2\text{SO}_4} + 0.059 \times \text{pH} + 0.7017\text{ V} \quad \dots\dots\dots \text{Eq. (1)}$$

Bulk electrolysis was performed in the H-cell reactor with a constant current (5 mA) in 0.1 M H_2SO_4 with 10 mM phenol. All solutions were purged with Ar for at least 20 minutes before the experiments.

4. Product analysis

The ECH products were qualitatively identified and quantitatively analyzed by gas

chromatography-mass spectrometry (GC-MS, QP2010Plus, Shimadzu) equipped with ZZS-5MS capillary column (30 m × 0.25 mm × 0.25 μm). High purity helium gas (He, 99.999%) was used as the carrier gas at a flow rate of 1.2 mL min⁻¹, and the split ratio was 40:1. The temperatures of the column oven and the inlet were set to 40 °C and 250 °C, respectively. The temperature program of the oven was set as the followings: began at 40 °C and maintained for 2 min; increased to 80 °C at a ramping rate of 10 °C min⁻¹ for 1 min, and increased to 200 °C with a ramping rate of 40 °C min⁻¹ for 5 min. Before gas chromatography analysis, the ECH product was extracted with dichloromethane and then injected into the gas chromatograph to avoid the destruction of the chromatographic column by water. Typically, 1 mL liquid was collected from the cathode reaction chamber after the electrolytic reaction, extracted three times with the same amount of 1 mL dichloromethane, and the organic phase was collected and dried with anhydrous sodium sulfate. A 0.22 μm needle filter was used to filter the organic phase prior to each analysis.

Then the quantitative results were calculated by using a standard calibration curve of phenol, cyclohexanone, and cyclohexanol solutions in 0.1 M H₂SO₄ with the same extraction method. The conversion, selectivity, and Faradaic efficiency (FE) were calculated according to the following equations:

$$Yield_{cyclohexanol} = \frac{n_{cyclohexanol}}{n_{phenol}} \times 100\% \quad \dots\dots\dots \text{Eq. (2)}$$

$$Yield_{cyclohexanone} = \frac{n_{cyclohexanone}}{n_{phenol}} \times 100\% \quad \dots\dots\dots \text{Eq. (3)}$$

$$Phenol \text{ conversion} = \frac{\text{mol of Phenol consumed}}{\text{mol of initial Phenol}} \times 100\% \quad \dots\dots\dots \text{Eq. (4)}$$

$$FE_{cyclohexanone} = \frac{4 \times n_{cyclohexanone} \times F}{Q} \times 100\% \quad \dots\dots\dots \text{Eq. (5)}$$

$$FE_{cyclohexanol} = \frac{6 \times n_{cyclohexanol} \times F}{Q} \times 100\% \quad \dots\dots\dots \text{Eq. (6)}$$

where $n_{cyclohexanol}$ and $n_{cyclohexanone}$ are the mole amounts of cyclohexanone and cyclohexanol after the reaction, F (=96485 C mol⁻¹) is the Faradaic constant, Q is the total charge passed in the experiments.

5. Materials Characterization

The morphologies and microstructures of the synthesized samples were investigated by scanning electron microscopy (SEM, Rigaku, Regulus8100) and transmission electron microscopy (TEM, FEI, Talos F200X) equipped with EDS (Super-X). X-ray powder diffraction (XRD) patterns were acquired on a Smart Lab 3KW (Rigaku, Japan) with a Cu K α radiation (60 kV, 60 mA) of $\lambda=0.154$ nm at room temperature. HAADF-STEM images were recorded on a Thermo Fisher Scientific TEM (Themis Z) working at 300 kV. X-ray photoelectron spectroscopy (XPS, Thermo Scientific) was carried out on an ESCALAB 250xi X-ray photoelectron spectrometer using Al K α as the exciting source, in which the binding energies were corrected referring to the binding energy of the C 1s peak at 284.8 eV. The electron paramagnetic resonance (EPR) was performed using a Bruker EMX X-Band ESR Spectrometer.

6. *In-situ* Raman measurements

Electrochemical in situ Raman spectroscopy was conducted using a Horiba LabRAM HR Evolution Raman spectrometer equipped with a custom-built spectro-electrochemical cell. The as-prepared electrodes were used as the working electrode, while a carbon rod and a Hg/Hg₂SO₄ electrode served as the counter and reference electrodes, respectively. The electrolyte was 0.1 M H₂SO₄. The *in-situ* Raman measurements were performed at applied potentials of -0.05 V vs. RHE and 0.00 V vs. RHE. A 633 nm laser was used for excitation, and Raman spectra were recorded at 0, 5, 30, and 60 min.

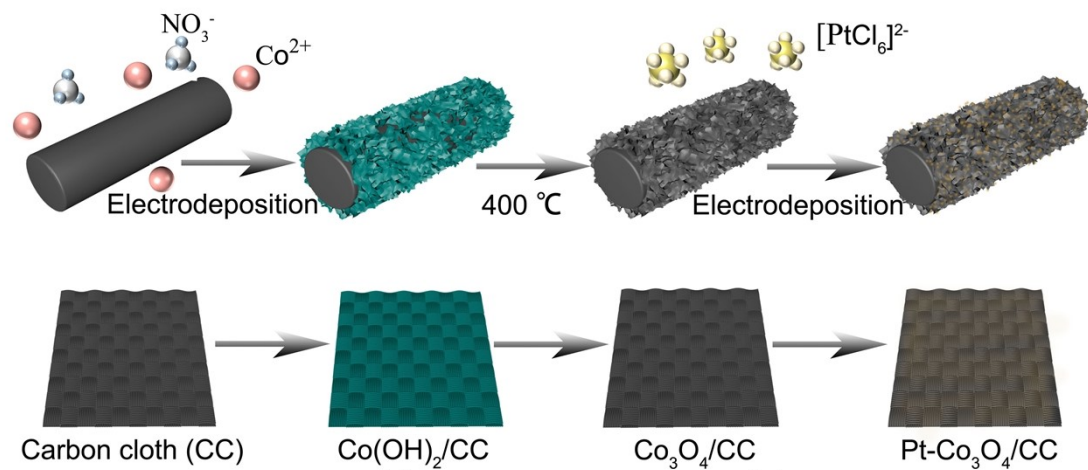


Figure S1. The schematic illustration of the fabrication of Pt-Co₃O₄ catalyst.

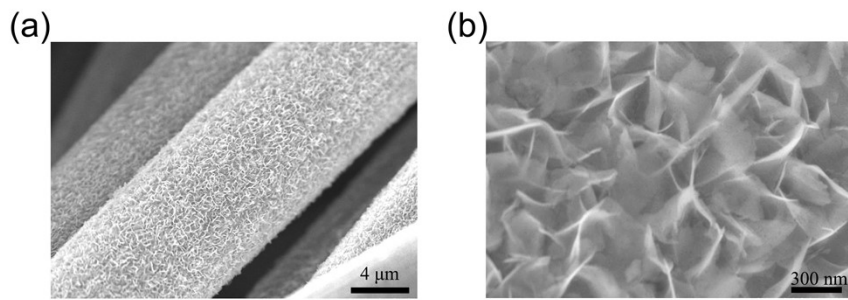


Figure S2. SEM images of Co_3O_4 nanosheets

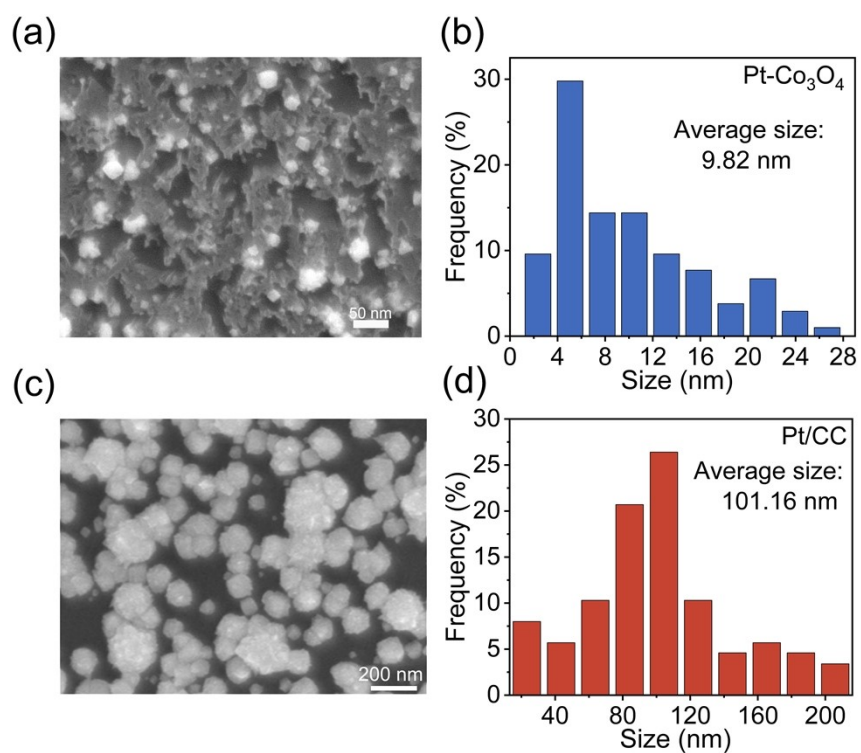


Figure S3. (a) Typical SEM image and (b) corresponding Pt particle size distribution histograms of Pt-Co₃O₄/CC. (c) Typical SEM image and (d) corresponding Pt particle size distribution histograms of Pt/CC.

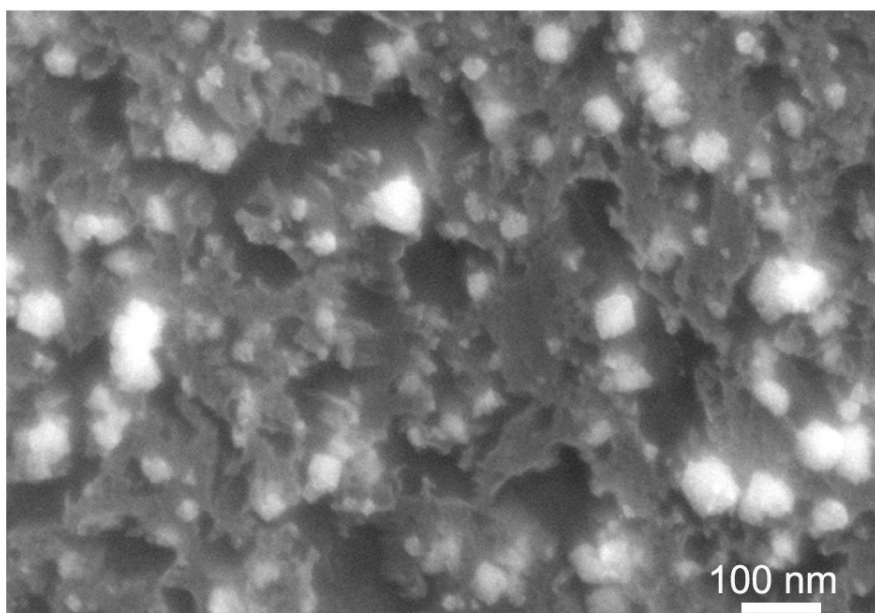


Figure S4. SEM image of the Pt-Co₃O₄ catalyst.

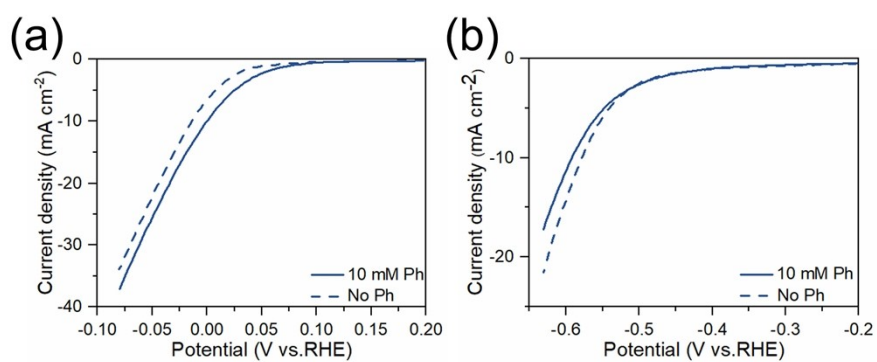


Figure S5. LSV curves for a) Pt and b) Co₃O₄ in 0.1 M H₂SO₄ with and without 10 mM Ph.



Figure S6. Standard curves of phenol, cyclohexanol, and cyclohexanone established by GC-MS analysis under identical conditions.

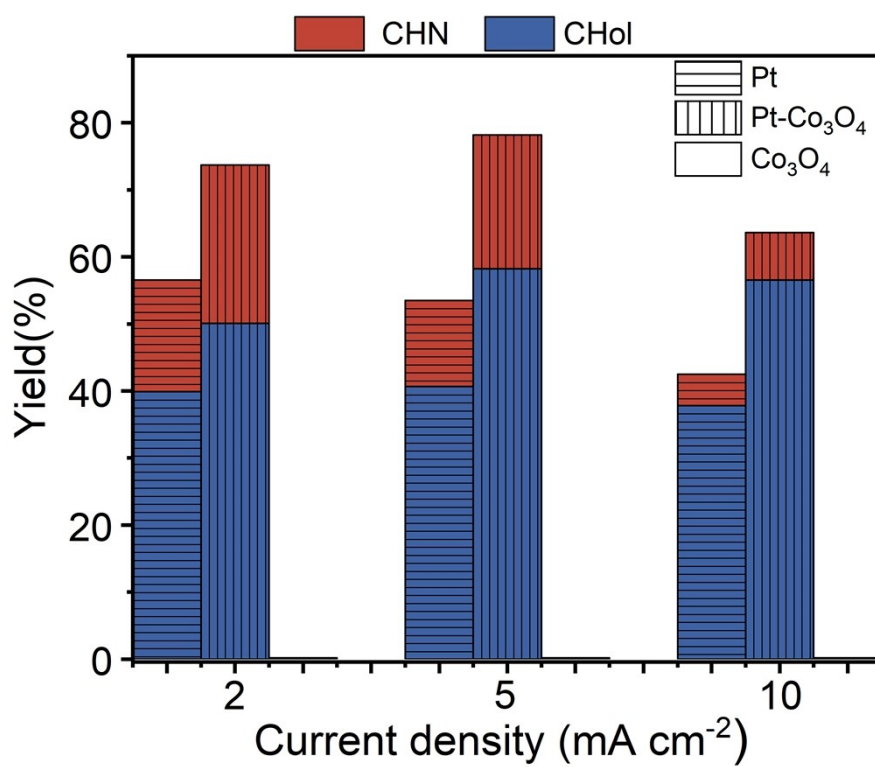


Figure S7. Comparison of product yield of cyclohexanol and cyclohexanone over Pt-Co₃O₄, Pt and Co₃O₄ under different current densities.

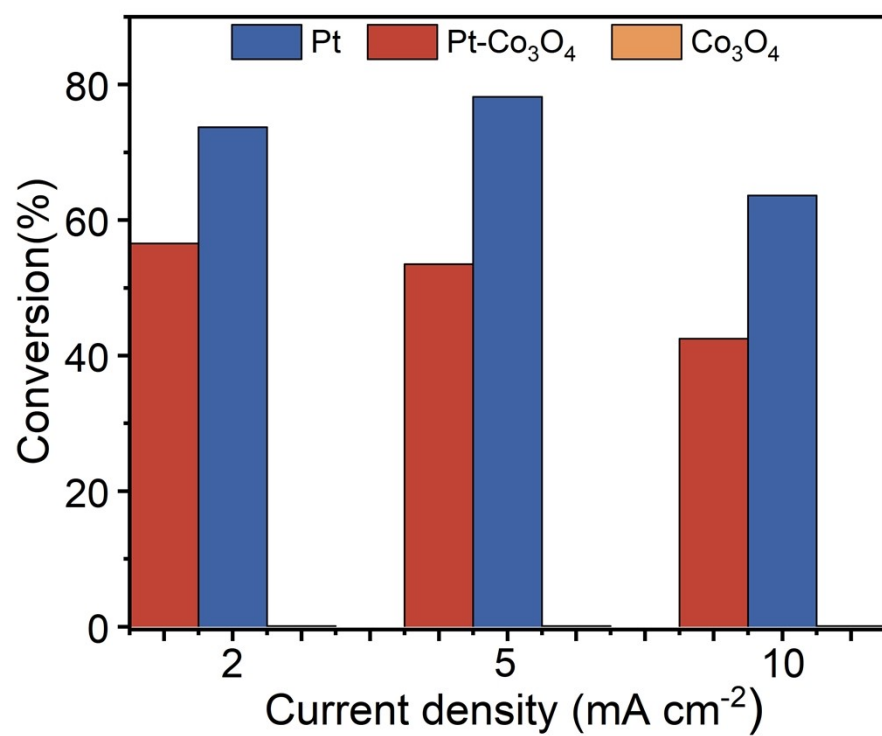


Figure S8. Comparison of phenol conversion over Pt-Co₃O₄, Pt and Co₃O₄ under different current densities.

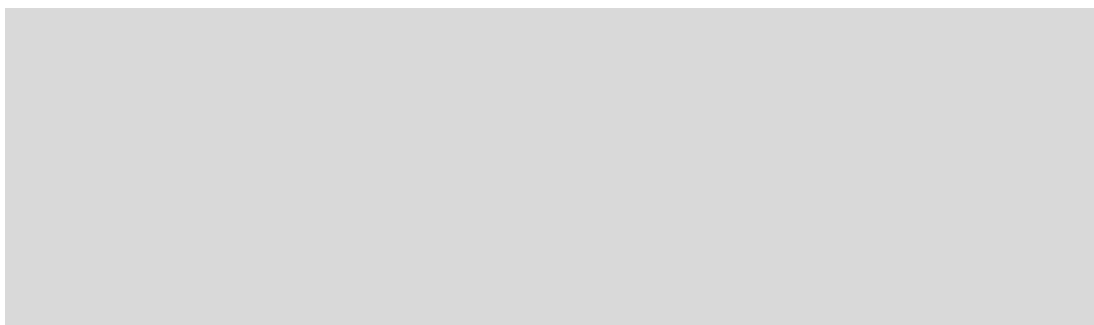


Figure S9. FEs of ECH over Pt-Co₃O₄ catalysts with different Pt deposition cycles at various current densities.

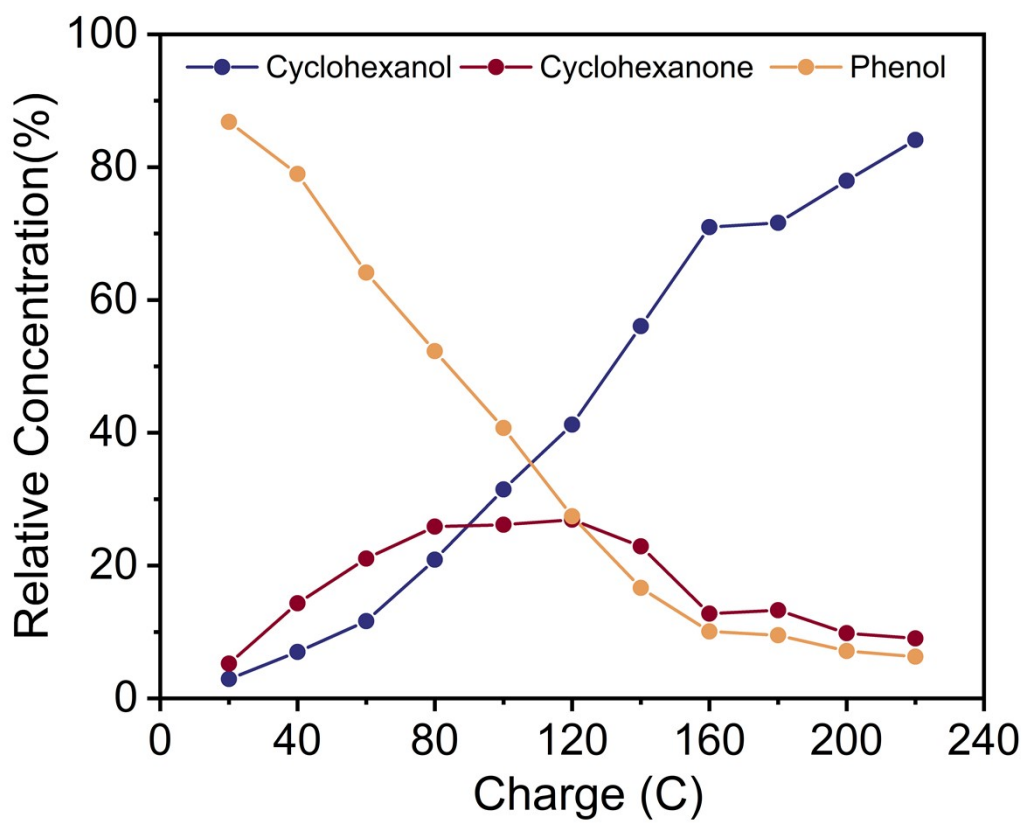


Figure S10. The concentration variation of phenol, cyclohexanol and cyclohexanone during electrolysis by Pt-Co₃O₄

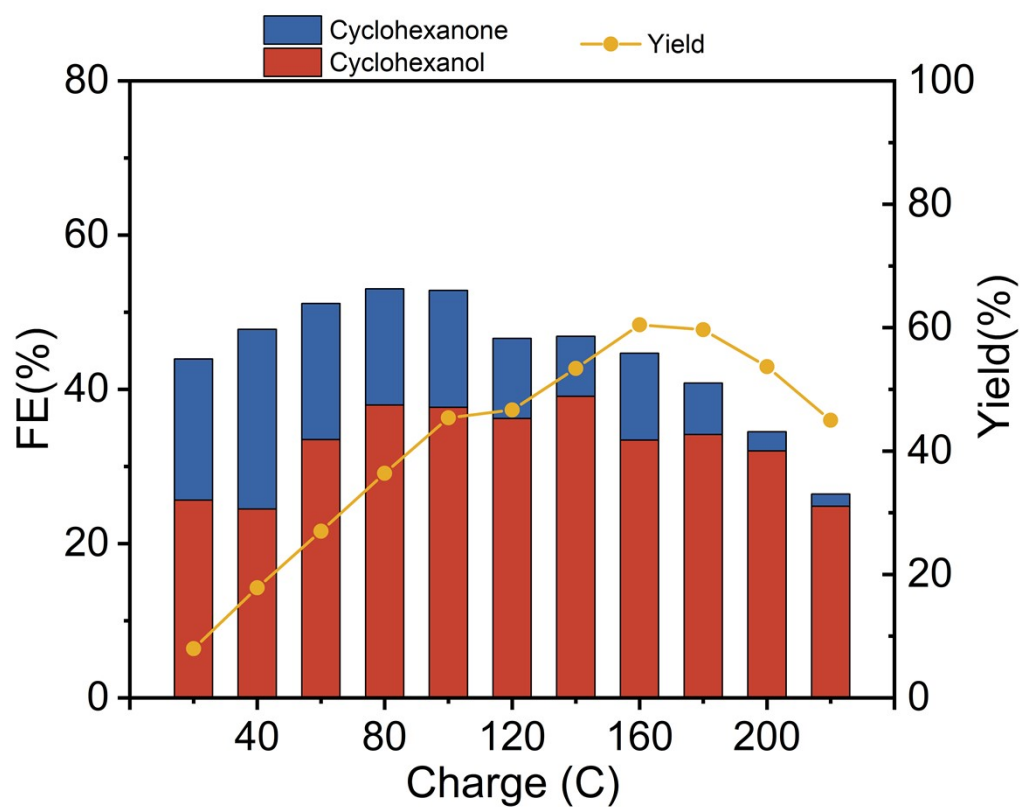


Figure S11. Yield of products and corresponding FEs vs charge in ECH of phenol over Pt/CC.

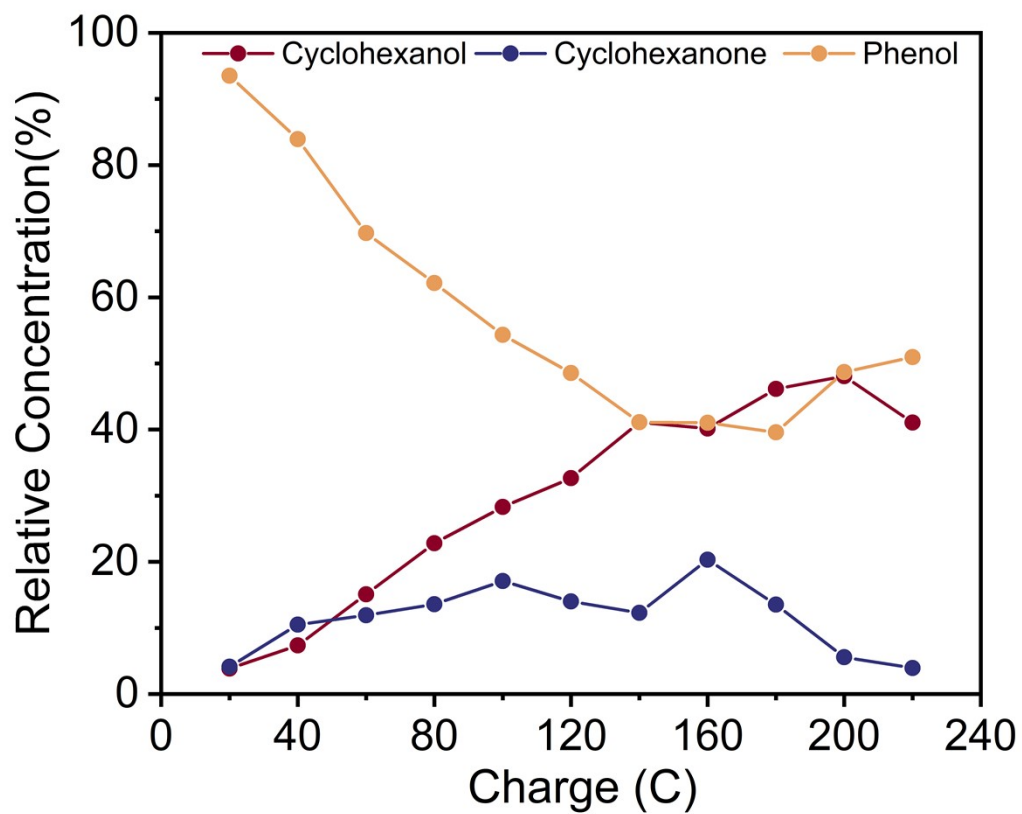


Figure S12. The concentration variation of phenol, cyclohexanol and cyclohexanone during electrolysis by Pt/CC.

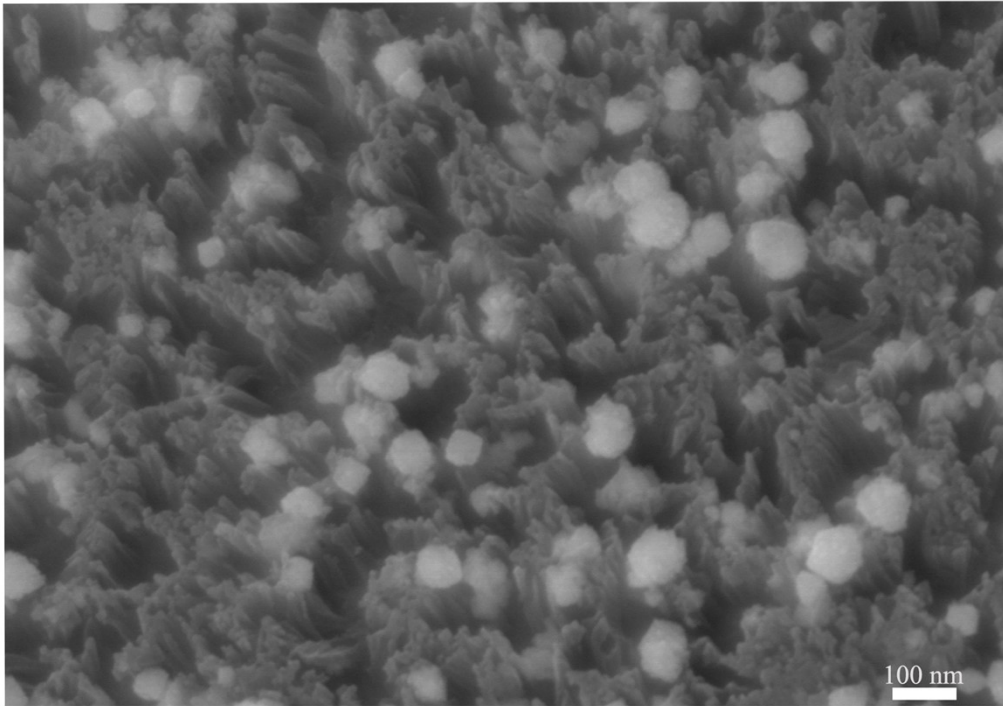


Figure S13. SEM image of Pt-Co₃O₄ after electrolysis.

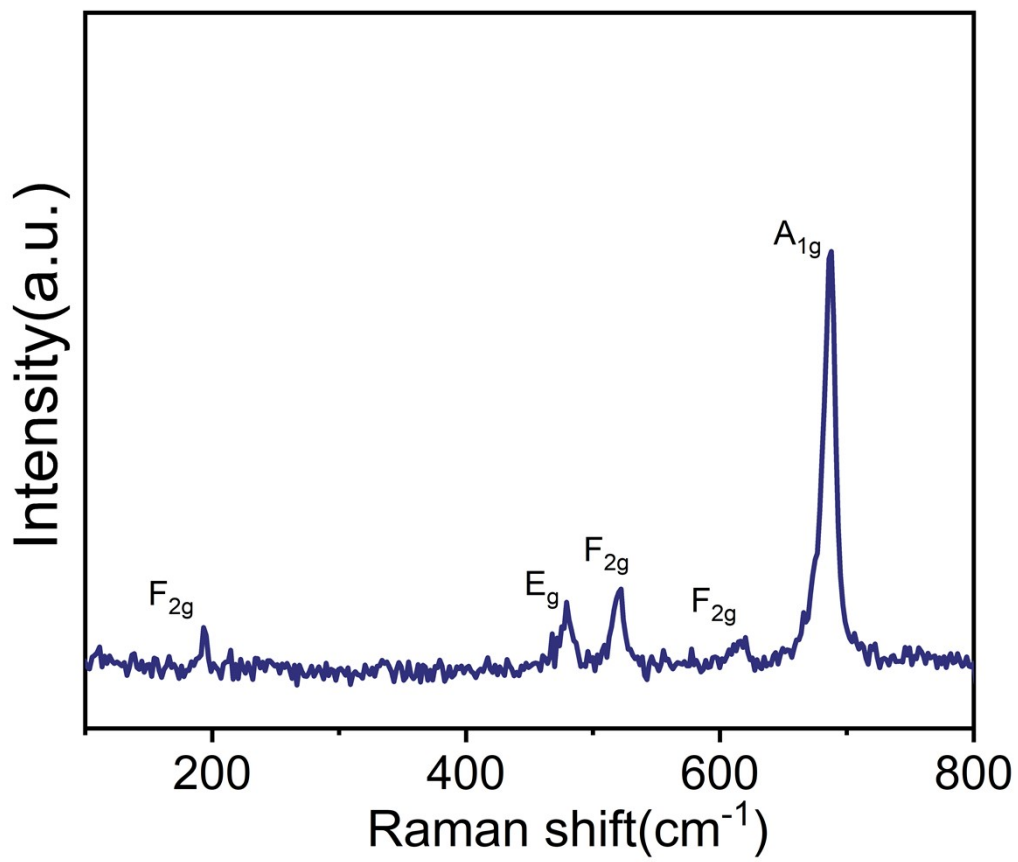


Figure S14. Raman spectra of Pt-Co₃O₄ after electrolysis.

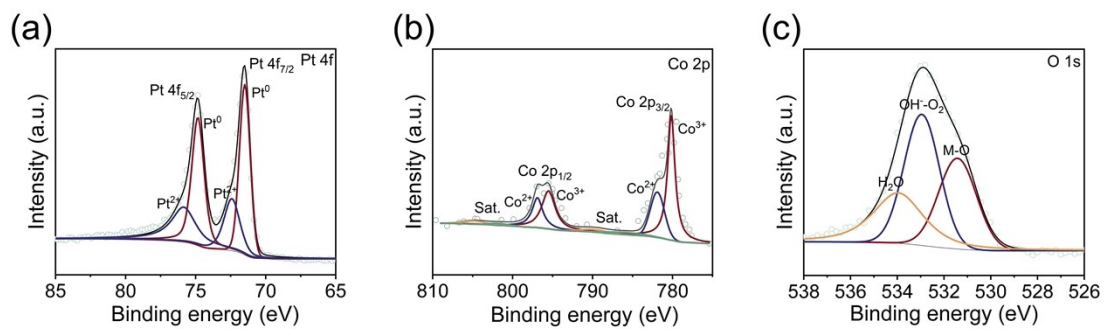


Figure S15. XPS spectra of Pt-Co₃O₄ after electrolysis.

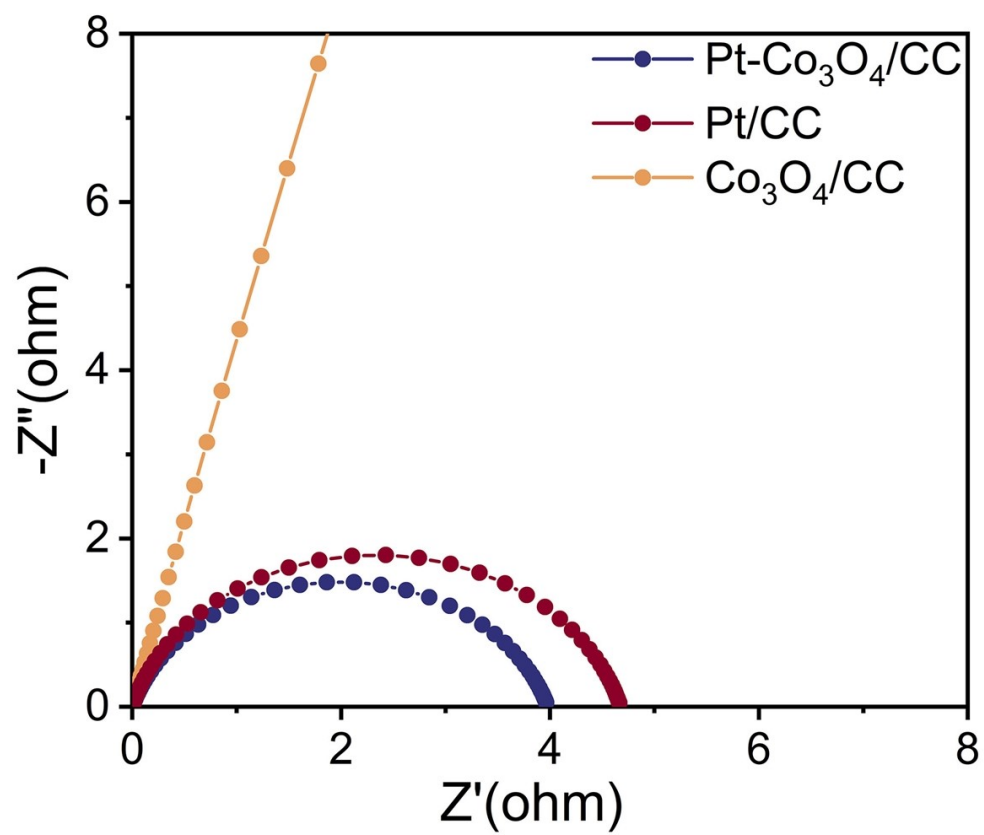


Figure S16. (a) Electrochemical impedance spectroscopy (EIS) of Pt-Co₃O₄, Pt/CC and Co₃O₄/CC.

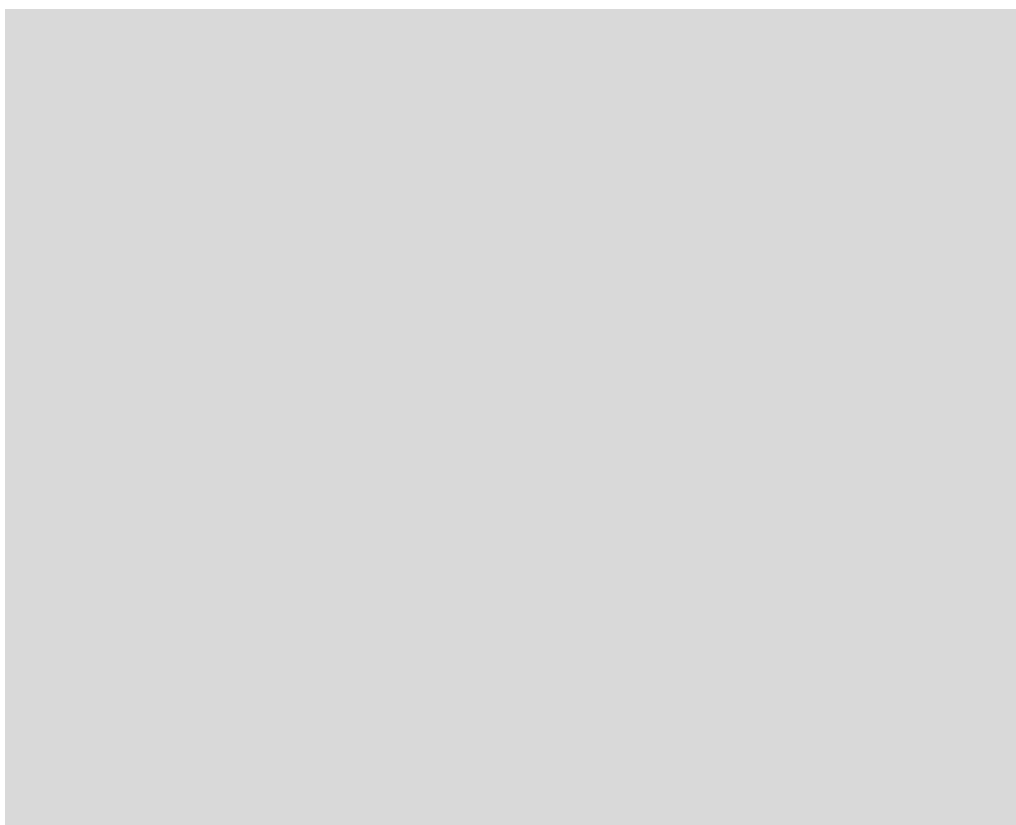


Figure S17. CV curves of Pt-Co₃O₄ and Pt in 0.1 M H₂SO₄ aqueous solution.

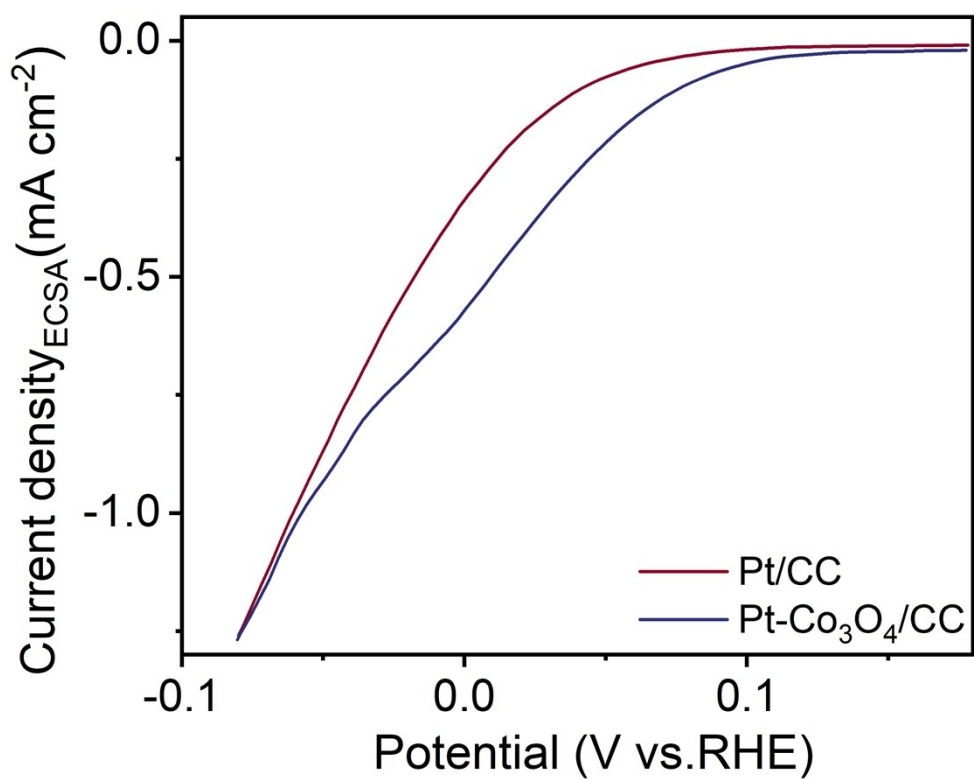


Figure S18. ECSA-normalized LSV curves of Pt-Co₃O₄ and Pt/CC for ECH of Ph to KA.

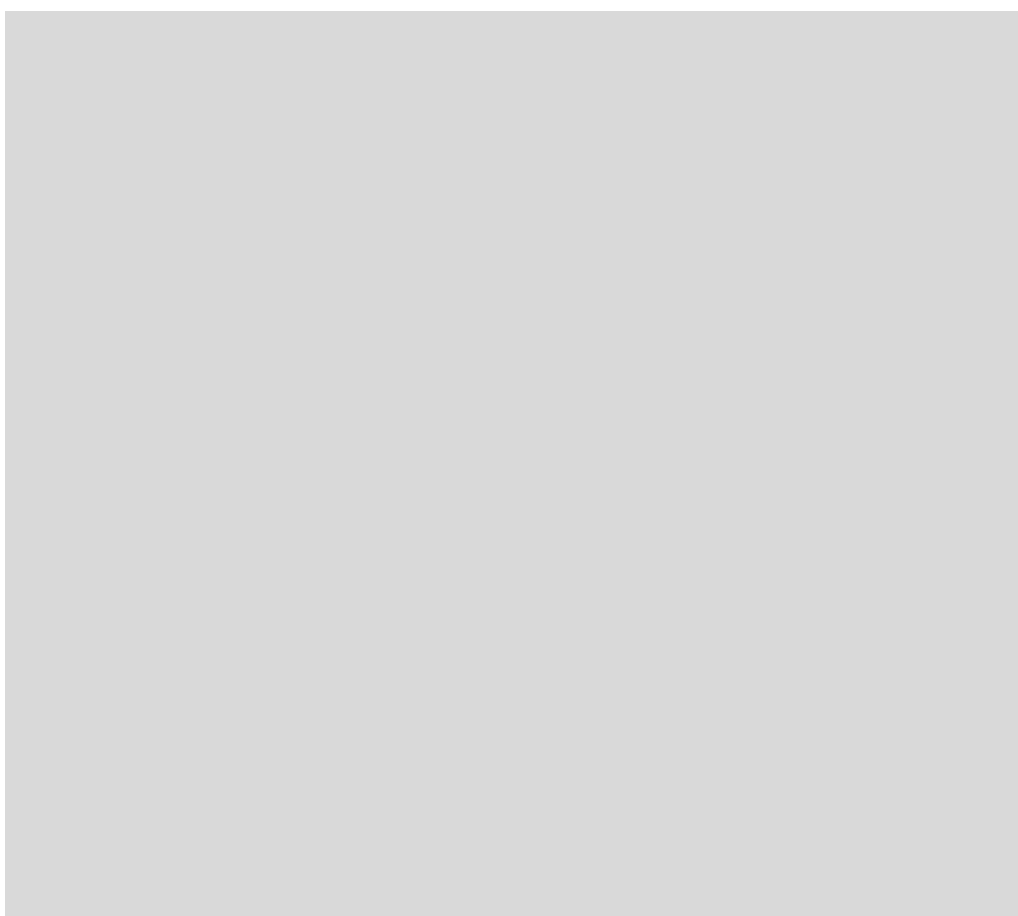


Figure S19. Open circuit potential (OCP) of Pt-Co₃O₄ and Pt/CC in 0.1 M H₂SO₄ solution before and after phenol was added.

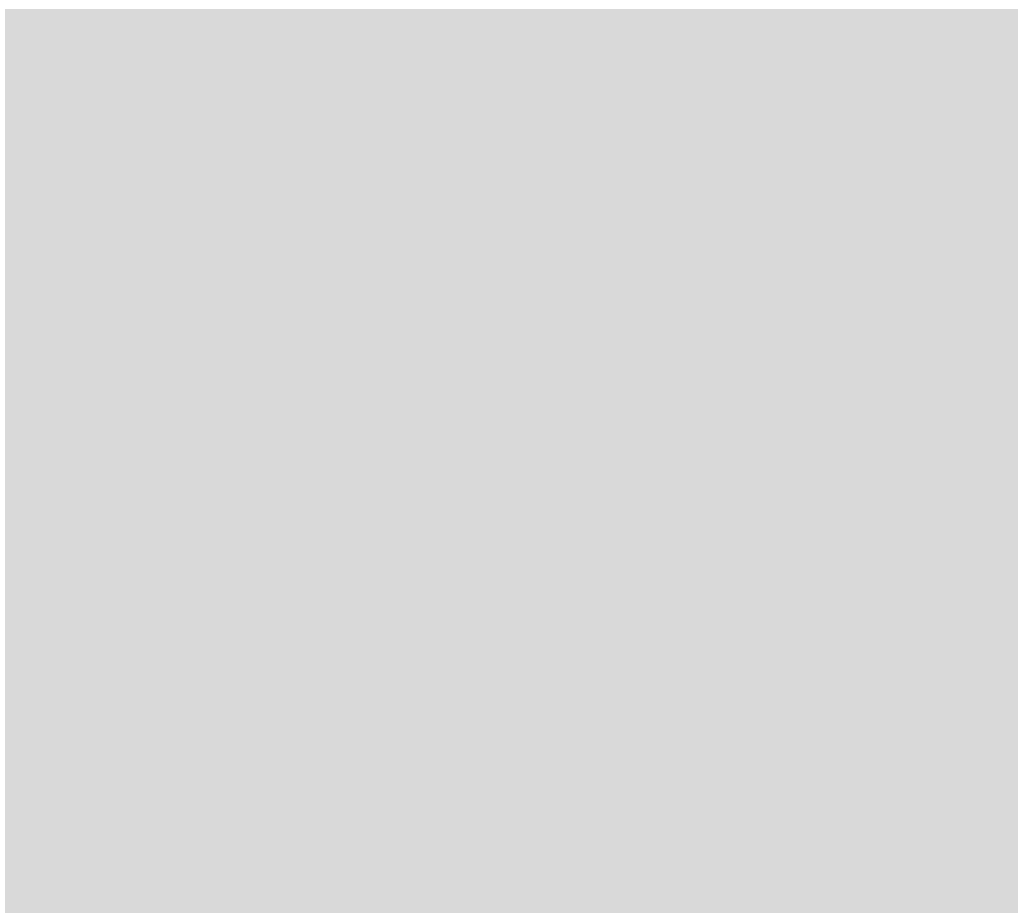


Figure S20. FTIR spectra of Pt-Co₃O₄, Pt/CC, Co₃O₄/CC samples after immersion in phenol solution.

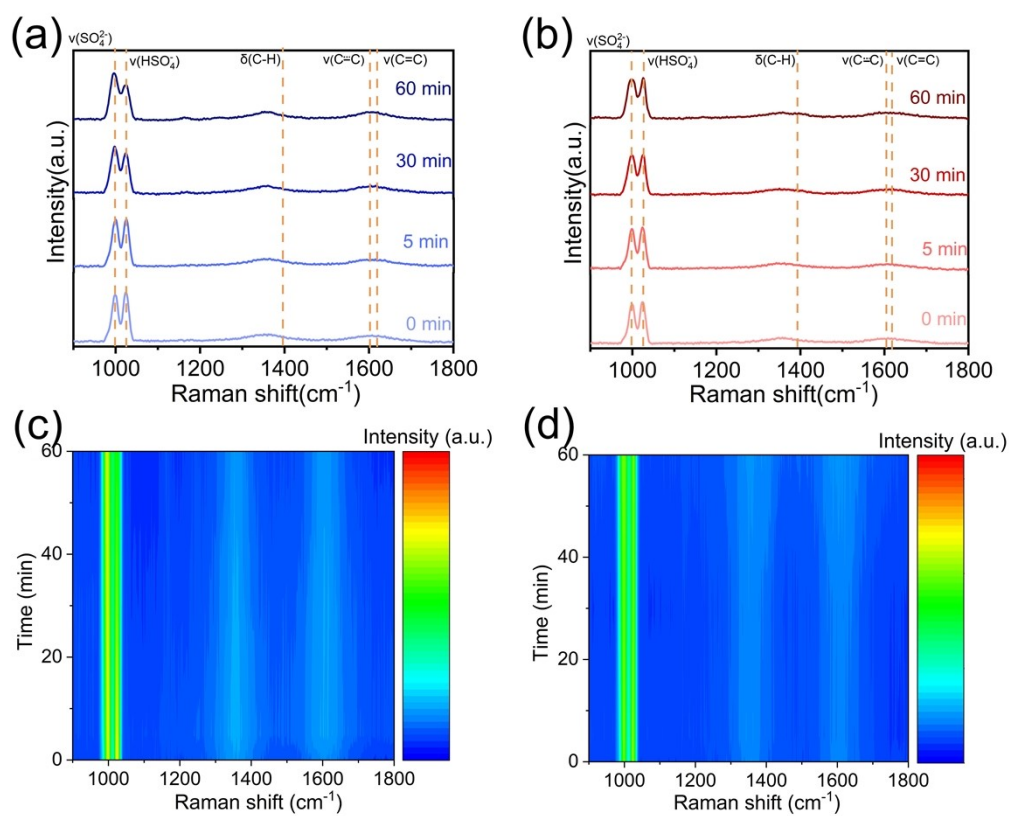


Figure S21. (a and c) *In situ* Raman spectra of ECH reaction recorded at 0, 5, 30 and 60 min. Reaction conditions: Pt-Co₃O₄ catalyst, 0.00 V (*vs.* RHE), 25 °C. (b and d) *In situ* Raman spectra obtained at 0, 5, 30 and 60 min under identical conditions using Pt/CC as the catalyst.

Table S1. The XPS results for O 1s.

Catalysts	Peak position (eV)	Peak area	Content (%)	O_V/O_L
Co ₃ O ₄	O _L (530.17)	O _L (18356)	O _L (53.5)	0.51
	O _V (531.46)	O _V (9369)	O _V (27.3)	
	O _{surf} (532.94)	O _{surf} (6597)	O _{surf} (19.2)	
Pt-Co ₃ O ₄	O _L (530.20)	O _L (15297)	O _L (41.5)	0.86
	O _V (531.57)	O _V (13281)	O _V (36.1)	
	O _{surf} (532.85)	O _{surf} (8258)	O _{surf} (22.4)	

Table S2. Comparison of ECH performance of Pt-Co₃O₄/CC electrode with that of other reported electrodes.

Entry	Catalysts	Electrolyte	T(°C)	Applied potential or Current density (mA cm ⁻²)	FE(%)	Yield(%)	Ref.
1	Pt-Co ₃ O ₄ /CC ^a	0.1 M H ₂ SO ₄ + 10 mM Ph	RT	5	71.4	93.2	This work
2	PtAu	0.2 M HClO ₄ + 10mM Ph	60	10	43	92	[1]
3	Pt ₃ RuSn	0.2 M H ₂ SO ₄ + 10mM Ph	50	22.2	39.5	91.5	[2]
4	Ni ₁₀ /MoO _{2-x} @C	0.1 M H ₂ SO ₄ + 20 mM Ph	60	2.5	53	95	[3]
5	Ni ₂₀ /MoO _{2-x} @C	0.1 M H ₂ SO ₄ + 20 mM Ph	60	1.8	49	86	[3]
6	Pt ₁ Rh ₁ /MCN ^a	0.2 M HClO ₄ + 10 mM Ph	RT	3.125	88	94	[4]
7	Ru/ACC	0.2 M HCl + 20 mM Ph	80	22.22	25	76	[5]
8	Pt/TiO ₂ ^b	0.1 M HClO ₄ + 20 mM Ph	25	6.2	33	74	[6]
9	PdRu/C	0.1 M Na ₂ SO ₄ +5 mM Ph	RT	0.6667	57.3	92.4	[7]
10	Pt ₃ Ru ₃	0.1 M H ₂ SO ₄ + 50 mM Ph	RT	10	60	100	[8]
11	Ru/TiO ₂	0.2 M phosphate buffer + 10 mM Ph	50	25	40	96	[9]

RT: room temperature; MCN: mesoporous carbon nanospheres; ACC: activated carbon cloth; SSB: shrimp shell biochar;

^aElectrolysis time corresponding to the theoretically complete conversion of phenol to cyclohexanol.

^bReaction for 15 h

Reference

- (1) Liu, F.; Gao, X.; Guo, Z.; Tse, E. C. M., Chen, Y., Sustainable Adipic Acid Production via Paired Electrolysis of Lignin-Derived Phenolic Compounds with Water as Hydrogen and Oxygen Sources. *J. Am. Chem. Soc.* **2024**, *146* (22), 15275-15285.
- (2) Du, Y.; Chen, X., Liang, C., Selective electrocatalytic hydrogenation of phenols over ternary Pt₃RuSn alloy. *mol. catal.* **2023**, *535*, 112831.
- (3) Zhou, P.; Guo, S.-X.; Li, L.; Ueda, T.; Nishiwaki, Y.; Huang, L.; Zhang, Z., Zhang, J., Selective Electrochemical Hydrogenation of Phenol with Earth-abundant Ni–MoO₂ Heterostructured Catalysts: Effect of Oxygen Vacancy on Product Selectivity. *Angew. Chem. Int. Ed.* **2023**, *62* (8), e202214881.
- (4) Zhou, L.; Zhu, X.; Su, H.; Lin, H.; Lyu, Y.; Zhao, X.; Chen, C.; Zhang, N.; Xie, C.; Li, Y.; Lu, Y.; Zheng, J.; Johannessen, B.; Jiang, S. P.; Liu, Q.; Li, Y.; Zou, Y., Wang, S., Identification of the hydrogen utilization pathway for the electrocatalytic hydrogenation of phenol. *Sci. China Chem.* **2021**, *64* (9), 1586-1595.
- (5) Garedew, M.; Young-Farhat, D.; Jackson, J. E., Saffron, C. M., Electrocatalytic Upgrading of Phenolic Compounds Observed after Lignin Pyrolysis. *ACS Sustain. Chem. Eng.* **2019**, *7* (9), 8375-8386.
- (6) Liu, Y.; Ji, K.; Wang, X.; Shi, Q.; Li, A.-Z.; Yin, Z.; Zhu, Y.-Q., Duan, H., Modulating the Coverage of Adsorbed Hydrogen via Hydrogen Spillover Enables Selective Electrocatalytic Hydrogenation of Phenol to Cyclohexanone. *Angew. Chem. Int. Ed.* **2025**, *64* (7), e202419178.
- (7) Liu, F.; Dai, Y.; Zhang, J.; Chen, W.; Liao, X.; Gu, C.; Wang, T.; Yin, Z.; Guan,

X., Han, B., Paired Pulse Electrocatalytic Conversion of Phenol for Co-Production of Cyclohexanol and Para-Benzoquinone. *Angew. Chem. Int. Ed.* **2025**, *64* (40), e202513889.

(8) Sun, Y.; Lv, Y.; Li, W.; Zhang, J., Fu, Y., Robust PtRu catalyst regulated via cyclic electrodeposition for electrochemical production of cyclohexanol. *J. Catal.* **2024**, *429*, 115219.

(9) Gu, Z.; Zhang, Z.; Ni, N.; Hu, C., Qu, J., Simultaneous Phenol Removal and Resource Recovery from Phenolic Wastewater by Electrocatalytic Hydrogenation. *Environ. Sci. Technol.* **2022**, *56* (7), 4356-4366.